ACTA ABP BIOCHIMICA POLONICA

Vol. 70, No 4/2023
843–853
https://doi.org/10.18388/abp.2020_6674

Regular paper

Modified Hongyu Decoction promotes wound healing by activating the VEGF/PI3K/Akt signaling pathway

Xiang Xu[1#], Wei-hua Yang[1#], Zhi-wei Miao[2], Chun-yu Zhang[2], Yi-jia Cheng[1], Yang Chen[1], Jin-gen Lu[3] and Ning He[1]

[1]Department of Anal-rectal Surgery, Zhangjiagang TCM Hospital Affiliated to Nanjing University of Chinese Medicine, Zhangjiagang, China; [2]Department of Gastroenterology, Zhangjiagang TCM Hospital Affiliated to Nanjing University of Chinese Medicine, Zhangjiagang, China; [3]Department of Anal-rectal Surgery, Longhua Hospital, Shanghai University of Traditional Chinese Medicine, Shanghai, China

Wound healing is a considerable problem for clinicians. Ever greater attention has been paid to the role of Chinese herbal monomers and compounds on wound healing. This study aims to elucidate the wound healing mechanism of Modified Hongyu Decoction (MHD) *in vivo* and *in vitro*. MHD wound healing activity *in vivo* was evaluated using an excision rat model. H and E staining, Masson's staining and immunofluorescence of wound tissue on days 7 and 14 were performed to evaluate the efficacy of MHD on wound healing. Subsequently, human umbilical vein endothelial cells (HUVECs) were used to evaluate wound healing characteristics *in vitro*. Cell Counting Kit-8 (CCK-8) and scratch assays were conducted to assess the effects of MHD on the proliferation and migration of HUVECs. The involvement of the VEGF/PI3K/Akt signaling pathway was assessed by western blotting. The rats in the MHD group displayed more neovascularization and collagen fibers. Western blotting of wound tissue showed that VEGF, PI3K, p-Akt and p-eNOS expression were significantly increased ($p<0.05$) in the MHD group. Cell Counting Kit-8 and scratch assays demonstrated that MHD promoted HUVECs proliferation and migration. MHD treatment significantly increased VEGF, PI3K, p-Akt and p-eNOS expression in HUVECs ($p<0.05$), which was inhibited by LY294002. Both *in vivo* and *in vitro* data indicated that MHD promotes wound healing by regulating the VEGF/PI3K/Akt signaling pathway.

Keywords: Modified Hongyu Decoction, wound healing, angiogenesis, VEGF/PI3K/Akt signaling pathway

Received: 16 February, 2023; revised: 07 July, 2023; accepted: 11 November, 2023; available on-line: 05 December, 2023

e-mail: huadongdaxiang@126.com

Acknowledgements of Financial Support: This work was supported by the Jiangsu Science and Technology Development Project of Traditional Chinese Medicine (QN202117), Natural Science Foundation of Nanjing University of Traditional Chinese Medicine (XZR2021056), Zhangjiagang Science and Technology Project (No. ZJGQNKJ202131), Science and Technology Project of youth Natural Science Foundation of Zhangjiagang TCM Hospital Affiliated to Nanjing University of Chinese Medicine (No. ZYYQ2008)

[#]Xiang Xu and Wei-hua Yang contributed equally to this work as Co-first authors.

Abbreviations: eNOS, endothelial Nitric Oxide Synthases; HPLC-Q-TOF/MS, high performance liquid chromatography coupled with quadrupole time-of-flight tandem mass spectrometry; HUVECs, human umbilical vein endothelial cells; MHD, Modified Hongyu Decoction; PI3K, PI3 kinase; rb-bFGF, recombinant bovine basic fibroblast growth factor; VEGF, vascular endothelial growth factor; VEGFR2, vascular endo-thelial growth factor receptor 2; α-SMA, alpha-smooth muscle actin

INTRODUCTION

Chronic and refractory wounds have become not only a major problem in the medical field, but also a challenge for doctors. Many factors, including chronic inflammation, diabetes mellitus and malignant tumors, can lead to delayed wound healing and even failure to heal. Indeed, millions globally suffer from chronic wounds. For example, a study from Germany in 2012 found that the prevalence of chronic nonhealing wounds was 1% to 2% in the general population (Heyer *et al.*, 2016). This not only affects their normal activities and reduces their quality of life, but also results in major social and economic problems. Care for such conditions has been reported to account for 2% to 3% of the healthcare budgets in developed countries (Frykberg & Banks, 2015; 2013; Richmond *et al.*, 2013). Many biological agents and dressings, containing a variety of growth factors, have been used to accelerate wound healing. However, there are also some complications, including the need for precise dosing to avoid the potential for excess scar formation and bioavailability (Zielins *et al.*, 2015). Additionally, these external treatments may cause adverse stimulation to the local wound, and changing wound dressings may cause unbearable pain for patients.

Wound healing is a dynamic and complex biological process, normally involving four phases: hemostasis, inflammation, proliferation and remodeling (Landen *et al.*, 2016). In the proliferative stage, neovascularization is an essential component of tissue repair, and also a key step of wound healing (Eming *et al.*, 2014; Shiojima & Walsh, 2002). Protein kinase B (Akt), a serine/threonine kinase, is a vital signal center for a wide range of cellular functions. PI3 kinase-dependent activation of Akt further affects the activity of several downstream pathways involved in cell proliferation, angiogenesis, senescence, apoptosis and cellular survival (Hoke *et al.*, 2016; Li & Wang, 2014). As upstream proteins of extracellular signaling, growth factors, including pro-angiogenic growth factors, activate many signaling pathways, including PI3K/Akt, which modulate several cellular activities involved in acute wound healing and maintenance of tissue homeostasis (Squarize *et al.*, 2010). Additionally, the bioactivities of pro-angiogenic growth factors are closely related to endothelial cell chemotaxis at the proliferative phase of angiogenesis and subsequently normal angiogenesis (Eming *et al.*, 2014; Zielins *et al.*, 2015). Among many pro-angiogenic growth factors, vascular endothelial growth factor (VEGF) is the most specific pro-angiogenic growth factor of the vascular endothelium (D'Alessio *et al.*, 2015). It activates the PI3K/Akt signaling pathway

after binding with VEGF receptor 2 (VEGFR2) on the cell membrane of endothelial cells, thereby participating in cell proliferation and angiogenesis (Olsson *et al.*, 2006).

Modified Hongyu Decoction (MHD) is composed of *Pulsatilla chinensis*, *Pseudostellariae radix*, *Sargentodoxa cuneate*, *Patrinia scabiosaefolia*, *Astragali radix* and *Cornus officinalis*. According to the theory of traditional Chinese medicine, it has the effect of clearing heat and toxic materials, benefiting qi for activating blood circulation. In clinical trials, MHD has been shown to have an outstanding effect on promoting wound healing. However, the underlying mechanisms have not been elucidated. Some active ingredients of MHD have been proved to protect wounds. Previous studies have reported that *A. radix* and its active ingredients, such as Astragaloside IV and Astragalus polysaccharide, promoted wound re-epithelization and angiogenesis and regulated extracellular matrix remodeling by enhancing VEGF expression and activating the PI3K/Akt signaling pathway (Zhang *et al.*, 2009; Chen *et al.*, 2012; Zhao *et al.*, 2017). Other active ingredients, for example, 5-hydroxymethylfurfural derived from processed *C. officinalis*, protected human umbilical vein endothelial cells (HUVECs) injured by high glucose and increased p-Akt protein expression (Cao *et al.*, 2013). Additionally, an aqueous extract of *Patrinia villosa* induced Akt phosphorylation and enhanced HUVECs proliferation and migration, consequently promoting angiogenesis (Jeon *et al.*, 2010). The above research indicated that the Akt signaling pathway may be the vital pathway for MHD to promote wound healing. Therefore, we investigated the therapeutic effect and the mechanism of MHD on wound healing *in vivo* and *in vitro* models.

MATERIALS AND METHODS

MHD preparation

The raw herbs for MHD were purchased from Beijing Tongrentang Co. Ltd (Beijing, China) (origin place of the raw herbs shown in Table S1 at https://ojs.ptbioch.edu.pl/index.php/abp/). *P. chinensis* 15 g (20180620), *P. radix* 15 g (200107), *S. cuneate* 30 g (20191204), *P. villosa* 30 g (200110), *A. radix* 30 g (20200214) and *C. officinalis* 15 g (20191218) were combined and submerged in distilled water (1000 mL) for 30 min. Subsequently, the mixture was extracted twice (1000 mL first followed by 500 mL) over 1 h. After two rounds of extraction, the resulting mixture was filtered. The filtrate was concentrated until the established drug content was 1.35 g/mL. To prepare the MHD extract used for cell experiments, 7.5 mL MHD (1.35 g/mL) was lyophilized using a LAB-1A-50E freeze dryer (Biocool, Beijing, China), yielding 2.02 g powder that was used in the *in vitro* study.

High-performance liquid chromatography of quadrupole time-of-flight mass spectrometry (HPLC-Q-TOF/MS) analysis of the main chemicals in MHD

For the qualitative analysis of the main ingredients in MHD, 0.2 mL MHD was extracted by adding 1 mL ethanol to a 1.5 mL tube. After 10 minutes of vortex, the mixture was centrifuged at 21 000×*g* for 5 min. The supernatant was collected and injected into a HPLC-Q-TOF/MS system which contained a Shimadzu UFLC 20ADXR system (Kyoto, Japan) and TripleTOF 5600 mass spectrometer (AB SCIEX, USA).

For the column separation, a Waters ACQUITY™ BEH C18 column (1.7 μm, 2.1×50; 1.7 μm) was used, and the column temperature was set at 35°C. Separation was achieved using a mobile phase of 0.02% formic acid-water as solvent A and acetonitrile as solvent B. The flow rate was 0.3 mL/min and the gradient elution program was as follows: 0–2 min, 10% solvent B; 2–30 min, 10–90% solvent B; 30–32 min, 90% solvent B; 32–33 min, 90–10% solvent B; 33–35 min, 10% solvent B. An aliquot of 2 μL supernatant was injected into this system. For the MS analysis, the elution was by ionization using the ESI source both in the positive and negative modes, which could acquire more MS data. In this study, the m/z scan for MS1 was set at a range of 50–1200, and for information-dependent acquisition, the MS2 range was 50–1000. The other parameters used in this study were as follows: ion source gases 1 and 2 were both 50 psi, DP was set at 55 eV, EP was set at 15 ev and the collision energy was 15 eV.

Experimental animals

Twenty-four healthy male Sprague-Dawley (SD) rats (175–195 g) purchased from the Medical Center of Suzhou University (Suzhou, China) (certificate no. SCXK (Su) 2017-0001) were used in this study. Before the experiments, all rats were adaptively fed for one week in polyethylene boxes with free access to autoclaved water and diet under controlled temperature (25°C) and a 12-h light/12-h dark cycle. All experiments were performed in adherence to the guidelines of the Institutional Animal Care and Use Committee of China and were approved by the Ethical Committee of Zhangjiagang TCM Hospital Affiliated to Nanjing University of Chinese Medicine (2021-08-89).

Incisional wound rat model and treatment

The rats were randomly assigned to the following four groups (n=6 rats/group): control group, recombinant bovine basic fibroblast growth factor (rb-bFGF) group (as the positive group), low-dose MHD (L-MHD) group, high-dose MHD (H-MHD) group. All rats were weighed and subsequently anesthetized by intraperitoneal administration of 2% pentobarbital sodium (30 mg/kg). The dorsal hair was shaved, the shaved area was disinfected with 75% alcohol and 2 cm-diameter full-thickness skin wounds were produced on the dorsum in the midline of the backs. The skin wound lost the epidermis, most of the dermis, the fat, and the panniculus carnosus-exposing the fascia layer (Amin *et al.*, 2015).

After surgery, surgical dressing was applied to the rats and the animals were maintained in individual cages. The L-MHD group was given 6.975 g/kg MHD, while the H-MHD group received 13.95 g/kg MHD by intragastric administration once daily. In the rb-bFGF group, each skin wound was topically given rb-bFGF (150 AU/cm^2, Zhuhai Essex Bio-Pharmaceutical Co., Ltd, Guangdong, China) three times daily. On days 7 and 14, three rats in each group were euthanized by overdose anesthesia (Li *et al.*, 2015), and the wound granulation tissue, liver and kidney were excised from each rat. A portion of the harvested tissue was immediately stored in liquid nitrogen, and the remaining tissue, liver and kidney were maintained in 10% buffered formalin for the following tests.

Wound contraction assay

On days 0, 3, 7, 10 and 14 after injury, an image of each wound area was obtained and measured. The percentage of wound contraction was calculated by the following equation (Amin *et al.*, 2015): wound contraction = (initial wound area − present wound area)/(initial wound area) ×100%.

Histological analysis

The wound tissues, liver and kidney tissues collected at different time points, and livers and kidneys collected after rats sacrificed in each group were fixed with 10% formalin, dehydrated, embedded in paraffin and cut into 5 μm sections. Hematoxylin and Eosin (H&E) staining and Masson trichrome staining were performed using staining kits (Solarbio Technology Co., Ltd, Beijing, China) according to the manufacturer's instructions. Wound healing characteristics, including new epithelium, granulation tissue and collagen deposition, were observed under an inverted microscope (Olympus CX43). Organ sections were stained with H&E for toxicity evaluation.

Immunofluorescence staining

Paraffin sections of wound tissue from days 7 and 14 were dehydrated with xylene and gradient ethanol and subsequently repaired with sodium citrate. Following three washes with 0.3% Triton in PBS to rupture the cell membranes, sections were blocked with immunofluorescence blocking solution for 1 hour at room temperature and incubated with CD31 (ab28364, 1:50, Abcam), α-SMA (#19245, 1:50, CST), VEGFR2 (#9698, 1:800, CST), CD34 (ab81289, 1:100, Abcam) antibodies overnight at 4°C. Subsequently, the sections were incubated with secondary antibodies, including Alexa Fluor 488 donkey anti-rabbit IgG antibody (Invitrogen, Carlsbad, USA) and Alexa Fluor 555 donkey anti-mouse IgG antibody (Invitrogen, Carlsbad, USA), for 1 hour at room temperature at a dilution of 1:800. Finally, slides were counterstained with DAPI for 10 min and were observed with a laser confocal microscope (Olympus, CKX53), with images obtained using LAS X software (Qimaging, USA).

Cell culture and treatment

Human umbilical vein endothelial cells (HUVECs) were purchased from FUHENG Biotechnology Co., Ltd (Shanghai, China) and identified by the American Type Culture Collection (ATCC; Manassas, VA, USA). The cells were cultured in Endothelial Cell Medium (ECM; FUHENG Biotechnology Co., Ltd, Shanghai, China) supplemented with penicillin (100 U/mL), streptomycin (100 μg/mL) and 15% (v/v) fetal bovine serum (FBS; Beijing Biological Industries Co., Ltd, China) and maintained at 37°C under 5% CO_2. After 3 passages, the cells were used for the experiments.

HUVECs were incubated with different MHD concentrations for 24 h. For blocking assay, HUVECs were treated with different concentrations of general PI3K/Akt inhibitor LY294002 (Sigma).

Cell proliferation assay

Cell proliferation was determined using the cell counting kit-8 (CCK-8) kit (MedChemExpress LLC, NJ, USA) according to the manufacturer's instructions. HUVECs (2×10^4 cells, 100 μL per well) with ECM containing 15% FBS were seeded in 96-well plates and incubated for 24 hours at 37°C under 5% CO_2. The culture medium was replaced by ECM with 15% FBS and different MHD concentrations. For the control group, cells were continued incubation with ECM containing 15% FBS. The MHD concentrations were as follows: 0.1 μg/mL, 1 μg/mL, 5 μg/mL, 10 μg/mL, 50 μg/mL, 75 μg/mL, 100 μg/mL, 200 μg/mL, and 500 μg/mL. Following incubation at 37°C under 5% CO_2. After incubation of 24 hours, the CCK-8 solution was added to each well and incubated at 37°C in humidified 95% air and 5% CO_2 for a further 1 hour. The absorbance was determined at 450 nm for each well using a Microplate Reader (Bio-Rad, Hercules, CA, USA).

Scratch assay

The effect of MHD on HUVECs migration was assessed by the scratch assay (Liang *et al.*, 2007). HUVECs in ECM with 15% FBS were seeded into six-well plates (2×10^5 cells/well) and incubated at 37°C under 5% CO_2. When the cells reached approximately 80% confluence, three vertical scratch lines were made in each well using a 200 μL pipette tip, and cell debris was immediately washed out with phosphate-buffered saline (PBS). Subsequently, serum-free ECM (control) and serum-free ECM with MHD (5 μg/mL, 10 μg/mL, 25 μg/mL or 50 μg/mL) were added to the corresponding wells for 24 h of incubation at 37°C and 5% CO_2. Images of the scratches from the same areas in each well were obtained at 0 and 24 hours, respectively, using an inverted microphotograph (Olympus CX43, Tokyo, Japan) at a magnification of 40×. The scratch area was measured using the Image-J software (NIH, USA).

Western blot

Wound tissues or HUVECs were lysed using lysis buffer with RIPA Lysis Buffer, Phenylmethanesulfonyl fluoride (PMSF), Ethylene Diamine Tetraacetic Acid (EDTA) and protease and phosphatase inhibitor. Total protein concentrations were then quantified using the BCA protein assay kit (Thermo Fisher Scientific, Waltham, USA). Subsequently, equal amounts of proteins were separated by 10% sodium dodecyl sulfate-polyacrylamide gel electrophoresis (SDS-PAGE) and transferred to polyvinylidene difluoride membranes (Millipore, Burlington, MA, USA) using a transfer system (Bio-Rad). After blocking in blocking solution for 1 hour at room temperature, the membranes were incubated overnight at 4°C with primary antibodies diluted in primary antibody dilution buffer, followed by incubation with the horseradish peroxidase-conjugated secondary antibodies for 1 hour at 37°C. The antibodies included anti-phosphorylate Akt (p-Akt, #4060, 1:1000, CST), anti-Akt (#4685, 1:1000, CST), PI3K (#4249, 1:1000, CST), VEGFR2 (#9698, 1:1000, CST), anti-phospho-eNOS (p-eNOS, ab215717, 1:1000, Abcam), anti-β-actin (ab8227, 1:5000, Abcam), horseradish peroxidase-conjugated anti-rabbit IgG (1:5000) and anti-mouse IgG (1:5000). Immunosignals were detected using a chemiluminescence detection kit (Millipore, Burlington, MA, USA) and a gel imaging system (Tanon Science&Technology Co., Ltd., Shanghai, China). β-actin was used as an internal reference. The signal intensity was quantified using Image-J software.

Statistical analysis

For statistical analysis, all data values were analyzed and calculated using GraphPad Prism 8.0 (GraphPad Software Inc., San Diego, CA, USA) and expressed as

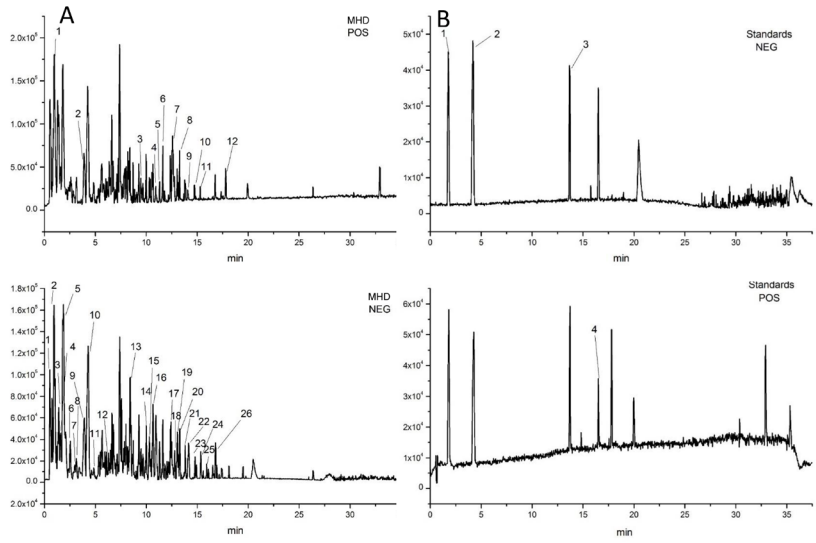

Figure 1. Total ion chromatography of the standards and the Modified Hongyu Decoction (MHD) in negative/positive mode by HPLC-Q-TOF/MS.

mean ± standard error of the mean (SEM) of three determinations. The data analysis was performed by one-way analysis of variance (ANOVA) followed by Dunnett's test, and $p<0.05$ was considered statistically significant.

RESULTS

HPLC-Q-TOF/MS analysis of MHD

MHD consists of six herbs that are commonly used in China. For the qualitative analysis of the MHD, we constructed an in-house component library of the MHD, then we compared the MS1 and MS2 data with the literature or the standard solutions. Figure 1 shows the total ion chromatography of the standards and the MHD. The main chemical components in MHD detected by HPLC–Q-TOF/MS are shown in Table S2 at https://ojs.ptbioch.edu.pl/index.php/abp/.

Changes in body weight and hepatorenal toxicity in rats after MHD administration

During the entire experiment, the body weight of all the rats increased gradually. There was no significant difference in body weight among the four groups, which demonstrated that MHD did not affect body weight (Fig. 2A). H&E staining of rats' liver and kidneys showed that, compared with the control group, there were no significant pathological changes in the MHD treatment groups, which indicated that MHD has no hepatorenal toxicity (Fig. 2B).

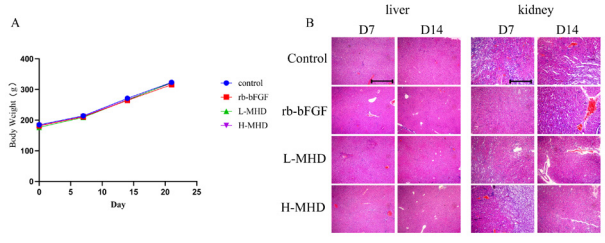

Figure 2. Changes in body weight and hepatorenal toxicity in rats after Modified Hongyu Decoction (MHD) administration.
(**A**) The body weight of each group was increased with time. (**B**) Representative images of H&E staining in the liver and kidney of each group were observed on days 7 and 14 (40× magnification, scale bar=100 μm).

MHD promoted wound healing *in vivo*

The wound areas of rats were observed, and images were obtained on days 0, 3, 7, 10 and 14. The representative images were combined and are presented in Fig. 3A. It was clear that the wound area in the four groups gradually decreased with time, indicating that the wounds were gradually healing. On day 7, the wound areas in the H-MHD and rb-bFGF groups were smaller than those in the control and L-MHD groups. On day 14, the wound areas in the H-MHD and rb-bFGF groups were almost healed, while the wound areas in the control and L-MHD groups were still apparent (Fig. 3A). Then, the wound areas were measured, and wound contraction of the designated days was plotted against post wounding days, as shown in Fig. 3B. From days 3 to 14, the percentages of wound contraction in the control group were respectively: 9.75%, 50.83%, 63.83% and 82.25%; and in the L-MHD group were respectively: 11.84%, 46.66%, 58.07% and 87.96%; H-MHD group were respectively: 11.84%, 77.94%, 93.18% and 99.52%; and the rb-bFGF group were respectively: 20.89%, 77.93%, 87.26% and 99.11%. On days 7, 10 and 14, the percentages of wound contraction in the H-MHD and rb-bFGF groups were significantly increased compared with the control and L-MHD groups. There was no significant difference in the percentages of wound contraction between the H-MHD and rb-bFGF groups (Fig. 3B). In general, MHD treatment promoted wound healing in rats.

MHD improved wound granulation tissue *in vivo*

H&E staining showed less inflammatory infiltration in the rb-bFGF and H-MHD groups compared with the control and L-MHD groups on day 7 (Fig. 4A). On day 14, epithelial layer regeneration in the H-MHD group

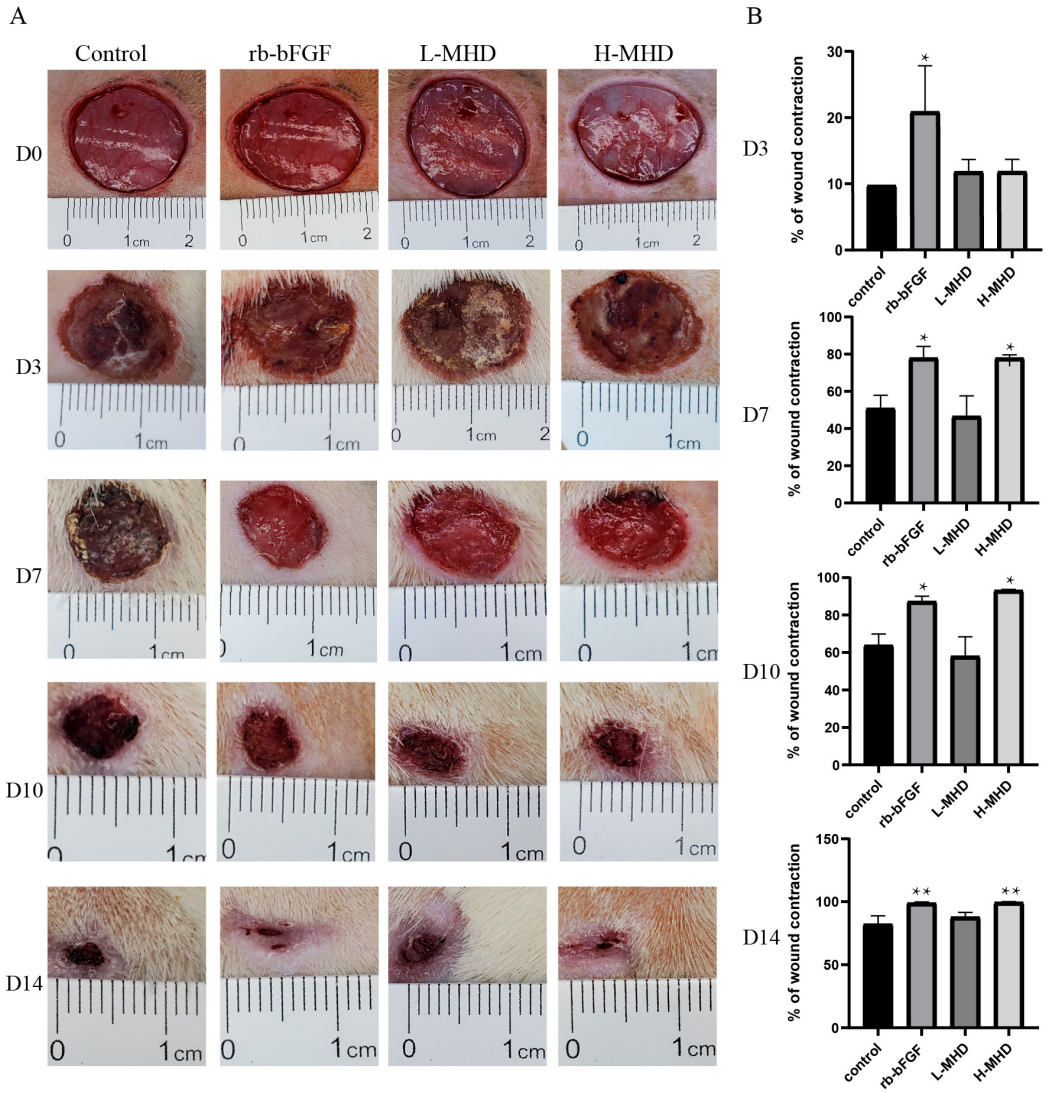

Figure 3. Modified Hongyu Decoction (MHD) promoted wound healing *in vivo*.
(**A**) Representative images of wound areas in each group on days 0, 3, 7, 10 and 14. (**B**) Percentage of wound contraction of the different groups on days 0, 3, 7, 10 and 14; n=3, $^{*}p<0.05$, $^{**}p<0.01$, compared with the control group.

was thicker and more complete than in the other groups (Fig. 4A). Masson's staining revealed more collagen fibers in the wounds treated with rb-bFGF or H-MHD than the control and L-MHD groups on both days 7 and 14 (Fig. 4B). These data indicated that H-MHD was almost comparable with rb-bFGF in promoting wound closure, particularly during the later wound healing stage. In conclusion, MHD significantly increased wound closure in rats in a dose-dependent manner.

MHD enhanced angiogenesis in the wound areas of rats

The quantification of new blood vessel density was defined as the ratio of the number of VEGFR2-, CD31-, CD34- and α-SMA-positive staining to DAPI per field. As shown in Fig. 5, both on days 7 and 14, the number of VEGFR2-, CD31-, CD34- and α-SMA-positive staining were rarely observed in the control and L-MHD groups, whereas significantly more positive staining was seen in the rb-bFGF and H-MHD groups (Fig. 5A–B). The quantification showed that both rb-bFGF and H-MHD augmented the production of VEGFR2, CD31, CD34 and α-SMA in the wound areas in rats, and there was no significant difference between these two groups (Fig. 5C–D). The results demonstrated that MHD could enhance angiogenesis in the wound areas of rats.

MHD activated the VEGF/PI3K/Akt signaling pathway *in vivo*

To investigate molecular mechanisms underlying the therapeutic efficacy of MHD on dorsal full-thickness excisional wounds in rats, we evaluated the expression of proteins related to the VEGF/PI3K/Akt signaling pathway by western blotting. Both on days 7 and 14, the protein expression levels of VEGFR2, PI3K, p-Akt and p-eNOS in the H-MHD and rb-bFGF groups were significantly ($p<0.05$) higher than those in the control and L-MHD groups, whereas no significant differences were observed between the H-MHD and rb-bFGF groups (Fig. 6A–B). These results demonstrated that H-MHD activated the VEGF/PI3K/Akt signaling pathway *in vivo*.

MHD promoted HUVECs proliferation and migration

To determine the effect of MHD on the proliferation and migration of HUVECs, the CCK-8 assay, and

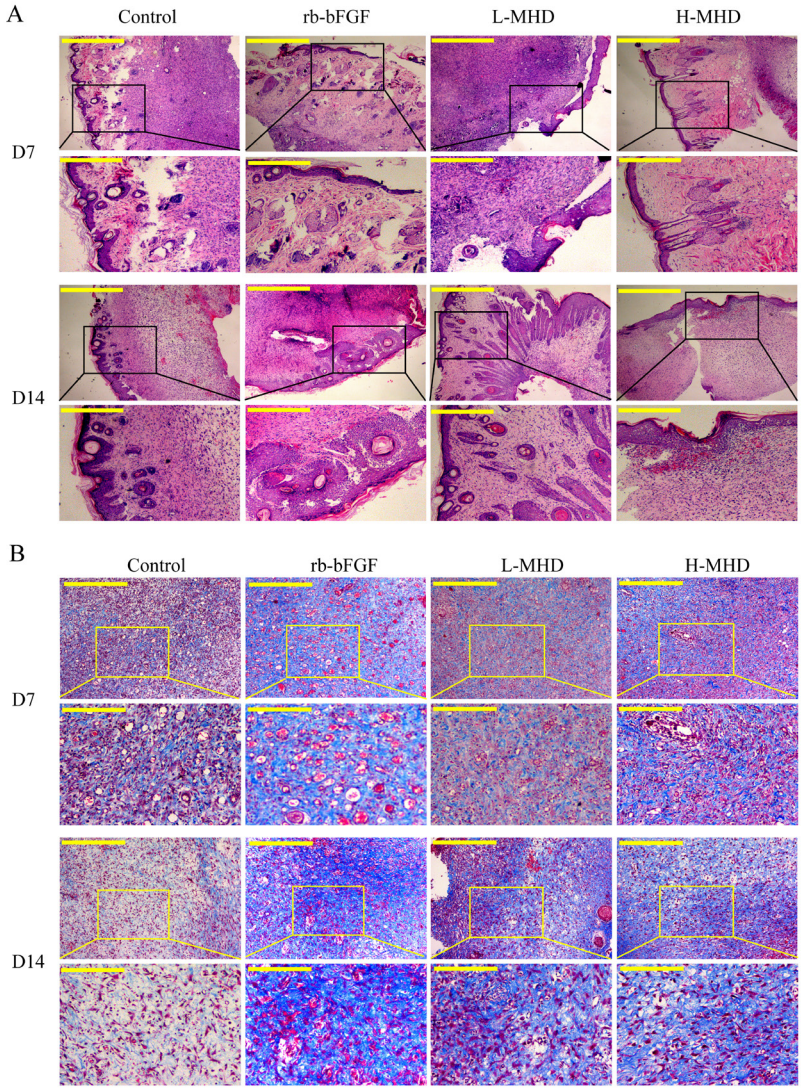

Figure 4. MHD improved wound granulation tissue *in vivo*.
(**A**) H&E staining was used to observe the wound tissues of each group on days 7 and 14 (upper: 40× magnification, scale bar=100 μm; lower: 200× magnification, scale bar=20 μm)n =3. (**B**) Masson's trichrome staining was used to analyze the changes in wound tissues of each groups on days 7 and 14 (upper: 40× magnification, scale bar=100 μm; lower: 200× magnification, scale bar=20 μm) n=3.

scratch assay were performed. The results showed that MHD promoted HUVECs proliferation in a concentration-dependent manner, and that the most potent stimulation was at 50 μg/mL (p<0.001) (Fig. 7A). As shown in Fig. 7B–C, the migration areas at 24 h at lower MHD concentrations (5 and 10 μg/mL) were respectively 18.30% and 20.03%, which was similar to that of the control group (11.42%) (Fig. 7B). Treatment with 25 μg/mL MHD clearly (p<0.05) reduced the wound width (31.62%), while treatment with 50 μg/mL MHD extensively (p<0.001) diminished the wound area (68.83%) at 24 h (Fig. 7B). 25 and 50 μg/mL MHD groups increased the migration rate of HUVECs compared with 5 and 10 μg/mL MHD groups (Fig. 7B). These data indicated that MHD accelerated the proliferation and migration of HUVECs in a concentration-dependent manner.

MHD activated the VEGF/PI3K/Akt signaling pathway in HUVECs

HUVECs were incubated with different MHD concentrations for 24 h, and the protein expressions related to the VEGF/PI3K/Akt signaling pathway were detected by western blot. MHD treatment increased the protein expression of VEGFR2, PI3K, p-Akt and p-eNOS of HUVECs in a concentration-dependent manner. The protein expressions of VEGFR2, PI3K, p-Akt and eNOS in the 50 μg/mL MHD treatment group were the highest among all concentrations of MHD groups (Fig. 8A).

Then, we observed the effects of different treatment times on the protein expression. The expression of VEGFR2, PI3K, p-Akt and p-eNOS protein at 5-30 min was increased in a time-dependent manner, while the expressions of protein were decreased at 60-120 min. The expressions of VEGFR2, PI3K, p-Akt and p-eNOS protein at 30 min of the treatment group were highest among all groups (Fig. 8B). Overall, these results indicated that MHD activated the VEGF/PI3K/Akt signaling pathway in HUVECs.

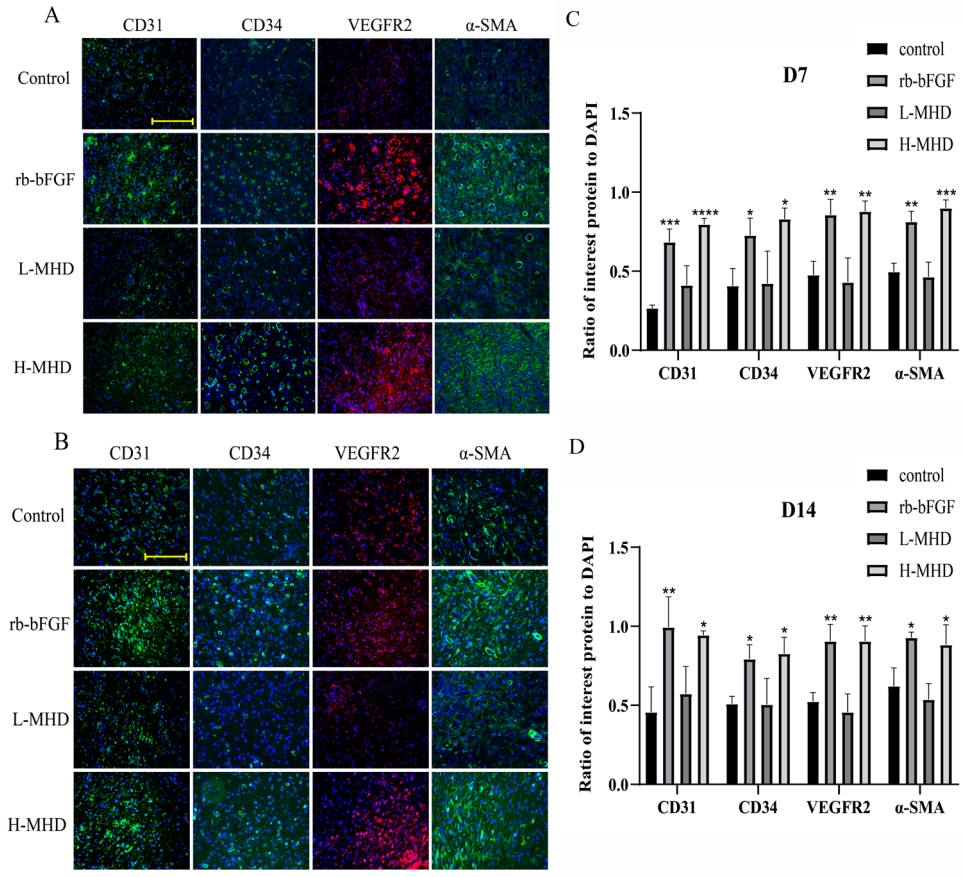

Figure 5. Modified Hongyu Decoction (MHD) enhanced angiogenesis in the wound areas of rats.
(**A–B**) CD31, VEGF, CD34 and α-SMA immunofluorescence staining of wound sections on days 7 and 14 (200× magnification, scale bar =100 μm) (**C–D**) Quantitative analysis of fluorescence intensity in CD31, VEGF, CD34 and α-SMA; n=3, $^{*}p<0.05$, $^{**}p<0.01$, $^{***}p<0.001$, $^{****}p<0.0001$, compared with the control group.

LY294002 reversed the effect of MHD on VEGF/PI3K/Akt signaling pathway in HUVECs

To further determine whether the angiogenic activity of MHD occurred through the Akt signaling pathway, LY294002 (a PI3K inhibitor) was used. After different concentrations of LY294002 treatment, the expression of PI3K, p-Akt, and p-eNOS were inhibited in a concentration-dependent manner, and the protein expression was significantly decreased after 20 μM and 50 μM

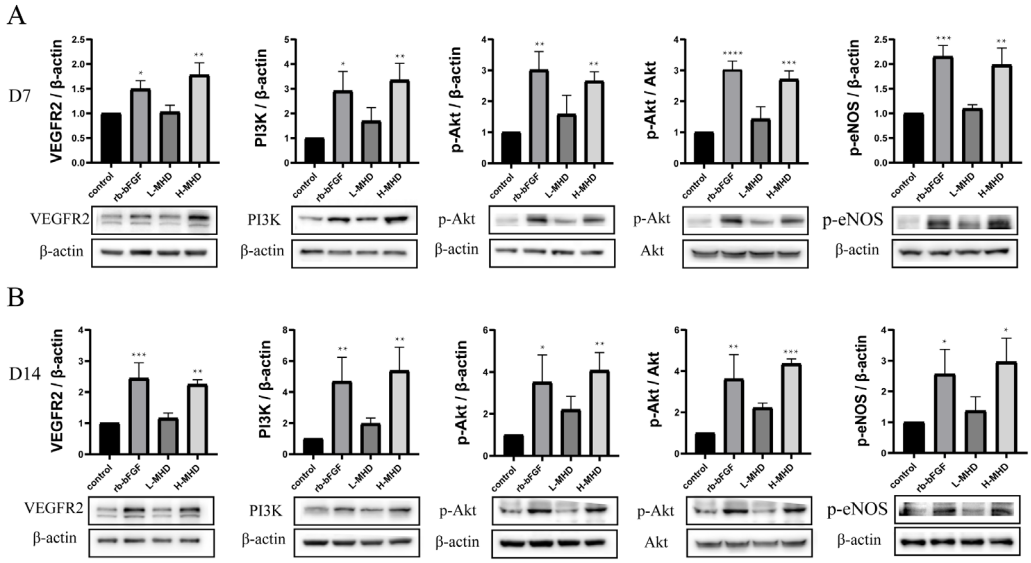

Figure 6. Modified Hongyu Decoction (MHD) activated the VEGF/PI3K/Akt signaling pathway *in vivo*.
(**A–B**) VEGFR2, PI3K and phosphorylation Akt (p-Akt) and eNOS *in vivo* on day 7 (**A**) and day 14 (**B**) were measured by western blot. Data shown in the graphs are representative of the mean ± SEM; n=3, $^{*}p<0.05$, $^{**}p<0.01$, $^{***}p<0.001$, compared with the control group.

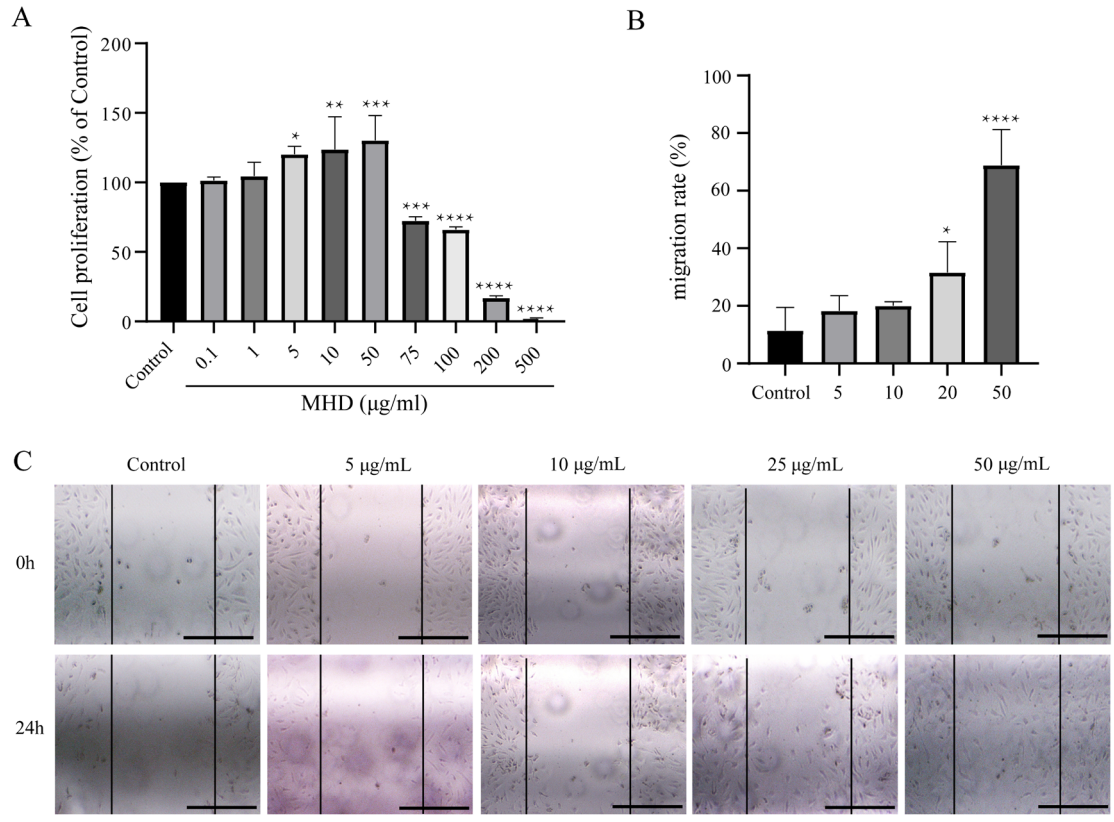

Figure 7. MHD promoted HUVECs proliferation and migration.
(**A**) HUVECs were incubated with different Modified Hongyu Decoction (MHD) concentrations (0.1–500 μg/mL) for 24 h. The concentration-dependent effect of MHD on cell proliferation was determined by the CCK-8 assay; n=3, $^{*}p<0.05$, $^{**}p<0.01$, $^{***}p<0.001$, $^{****}p<0.0001$, compared with the control group. (**B–C**) The wounds of HUVECs were created and then treated with MHD at 5–50 μg/mL for 24 h. The images were obtained at the same positions at time 0 h and after 24 h treatment with MHD (40× magnification, Scale bar = 100 μm), and cell migration rate was assessed by measuring the distance between the wound edges; n=3, $^{*}p<0.05$, $^{****}p<0.0001$, compared with the control group.

LY294002 treatment compared with 0 μM LY294002 (Fig. 9A). Then, 20 μM LY294002 was added to MHD treated HUVECs. MHD treatment increased the PI3K, p-Akt and p-eNOS protein expression and the p-Akt/Akt ratio in HUVECs. While LY294002 reversed the increasing of PI3K, p-Akt and p-eNOS protein expression and the p-Akt/Akt ratio induced by MHD (Fig. 9B). The results indicated that angiogenic activity of Modi-

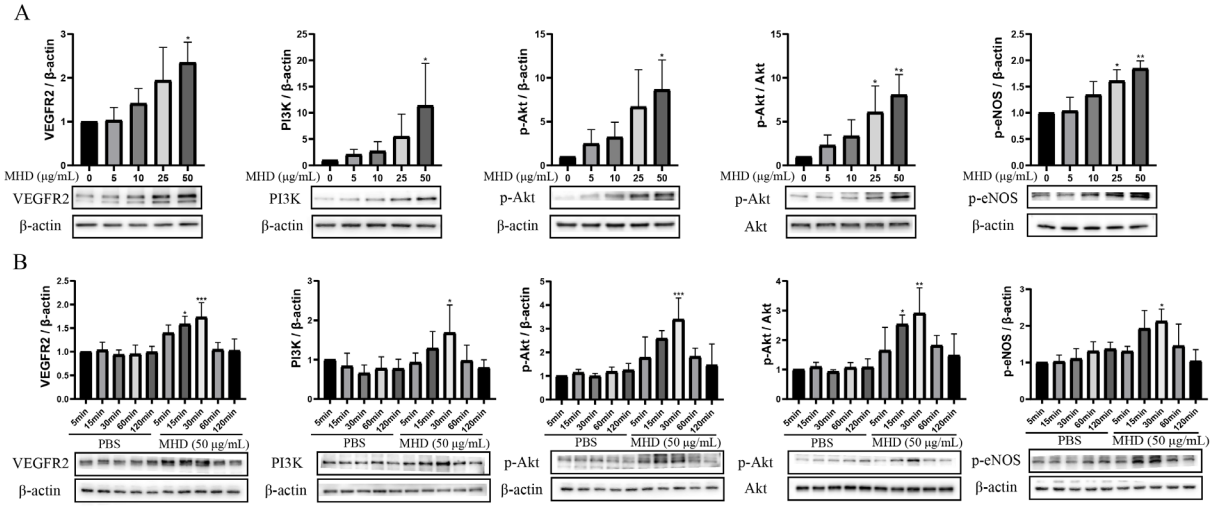

Figure 8. Modified Hongyu Decoction (MHD) activated the VEGF/PI3K/Akt signaling pathway in HUVECs.
(**A–B**) The effects of varying concentration (A, 5–50 μg/mL MHD for 30 min) and time (B, 50 μg/mL MHD for 5–120 min) of MHD on protein expression of VEGFR2, PI3K and p-Akt, Akt and p-eNOS in HUVECs were determined via western blot assay. Values shown are expressed as means ± SEM, n=3. For A, $^{*}p<0.05$, $^{**}p<0.01$ compared with the 0 μg/mL; For B, $^{*}p<0.05$, $^{**}p<0.01$, $^{***}p<0.001$, compared with the PBS group.

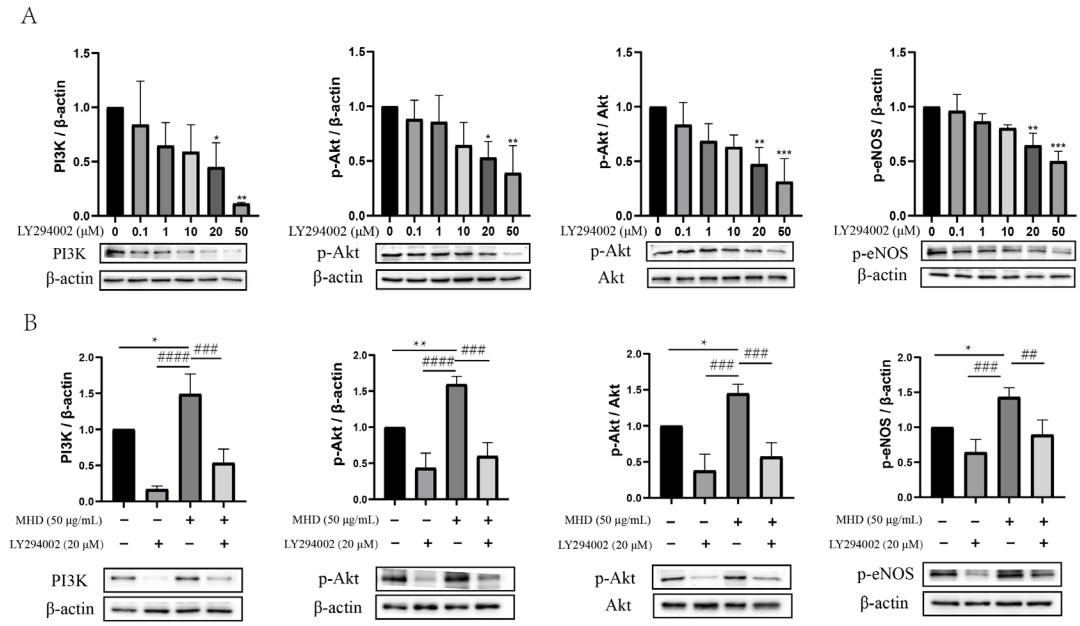

Figure 9. LY294002 reversed the effect of MHD on the VEGF/PI3K/Akt signaling pathway in HUVECs.
(**A**) HUVECs were incubated with different concentrations of LY294002 (0.1–50 μM) for 24 hours, and the protein expression of PI3K, p-Akt, Akt and p-eNOS was detected by western blot assay. n=3, $^{*}p<0.05$, $^{**}p<0.01$, compared with the 0 μM group. (**B**) HUVECs were incubated with LY294002 (20 μM) before the exposure to MHD (50 μg/mL)After 24 hours of incubation, the protein expression of PI3K, p-Akt, Akt and p-eNOS was detected by western blot assay. n=3, $^{*}p<0.05$, $^{**}p<0.01$, compared with the untreated cells; ##$p<0.01$, ###$p<0.001$, ####$p<0.0001$, compared with MHD-treated cells.

fied Hongyu Decoction (MHD) was responsible for the VEGF/PI3K/Akt signaling pathway.

DISCUSSION

When a wound occurs, granulation tissue composed of new ECM, newly formed blood vessels and fibroblasts will fill the wound bed (Gurtner *et al*., 2008). Neovascularization can provide oxygen and nutrition for the cells in the wound to maintain fibroblast proliferation, collagen synthesis and reepithelization (Zhang *et al*., 2016a; Eming *et al*., 2014), which is essential in wound healing. VEGF is a powerful stimulator of angiogenesis, which directly induces the proliferation and migration of endothelial cells (Simons *et al*., 2016; Breen, 2007). It is considered to be the key signal molecule of angiogenesis during wound healing (Barrientos *et al*., 2008). VEGF exerts biological effects by binding and activating VEGFR2 on the cell membrane (Terman *et al*., 1992; Eremina & Quaggin, 2004), after which several downstream signaling pathways, including the PI3K/Akt, IP3/Ca^{2+}/eNOS/NO, FAK, p38 mitogen-activated protein kinase and RAS/RAF-MEK/ERK pathways, can be activated (Olsson *et al*., 2006). Therefore, the PI3K/Akt pathway is defined to be a VEGF-related signaling pathway (Xu *et al*., 2014; Peng *et al*., 2016b; Ewald *et al*., 2014; Peng *et al*., 2016a), and it is the central pathway to control the angiogenesis process of endothelial cells (Somanath *et al*., 2006). Previous studies have shown that the PI3K/Akt signaling pathway is essential for the epithelial-mesenchymal transition and keratinocyte migration, and when dysfunctional, leads to compromised wound healing (Lee *et al*., 2012). Our study confirmed that MHD promotes wound healing by activating the VEGF/PI3K/Akt pathway *in vitro* and *in vivo*.

In the *in vivo* experiments, we observed that a high MHD dose promoted wound contraction, and the effect was equivalent to the rb-bFGF group. Histological analysis of wound tissues by H&E and Masson's staining confirmed that both the high MHD dose and rb-bFGF could decrease the number of inflammatory cells, facilitate granulation tissue formation and stimulate new blood vessels and collagen fiber formation. Moreover, H&E staining of the liver and kidney showed that MHD displayed no hepatorenal toxicity. We also labeled the markers of neovascular endothelial cells, such as VEGF, CD31, CD34 and α-SMA, using immunofluorescence. VEGF is an angiogenic factor which has high-efficiency and specific targeting characteristics for endothelial cells, and is closely associated with angiogenesis (Breen, 2007). It plays a key role in the initiation of angiogenesis and participates in the proliferation, migration, adhesion and permeability of vascular endothelial cells and other vascular wall components. VEGF promotes angiogenesis not only in physiological processes but also in inflammation, tumor, trauma and other conditions. CD31 is used to label endothelial cells and is expressed in normal blood vessels (Lertkiatmongkol *et al*., 2016). CD34 is a type I transmembrane glycoprotein, which is also widely used to label vascular endothelial cells (Lanza *et al*., 2001). α-SMA is mainly expressed in vascular smooth muscle cells and constitutes the contractile system of the vascular wall (Shinde *et al*., 2017). The results showed that VEGF, CD31, CD34 and α-SMA in the high MHD dose and rb-bFGF were greater than in the control group. These results confirmed that MHD promotes wound healing by stimulating angiogenesis.

Previous studies suggested that traditional Chinese medicine and extracts, including *Panax ginseng*, *Angelica sinensis*, *A. radix*, *Cinnamomum cassia* and *Salvia miltiorrhiza* among others, could be used as therapeutic agents for wound repair by stimulating angiogenesis and collagen synthesis (Majewska & Gendaszewska-Darmach, 2011). These effects were achieved by activating the VEGF/PI3K/Akt signaling pathway. A number of their monomer components have been shown to be involved in

promoting wound healing by regulating the PI3K/Akt signaling pathway. For example, cinnamaldehyde was reported to promote angiogenesis and wound healing by upregulating the PI3K signaling pathway (Yuan *et al.*, 2018). One of the active ingredients of MHD, astragaloside IV, has also been reported to significantly stimulate angiogenesis through the PI3K/Akt signaling pathway (Zhang *et al.*, 2011). Using western blotting, we also found that a high MHD dose increased VEGF secretion, activated PI3K and induced the phosphorylation of Akt and its downstream target eNOS, thus promoting new blood vessel formation. There are also some reports in the literature about the effect of compounds on wound healing. For example, *Danggui Buxue* extract-loaded liposomes in thermosensitive gel enhanced *in vivo* dermal wound healing via activation of the VEGF/PI3K/Akt and TGF-β/Smads signaling pathways (Cui *et al.*, 2017). These studies were similar to our results and demonstrated that MHD has the potential to promote angiogenesis through the VEGF/PI3K/Akt signaling pathway and is beneficial for wound healing.

HUVECs are frequently used as an *in vitro* model of angiogenesis, as angiogenesis requires endothelial cell migration and morphogenesis (Li *et al.*, 2017). In this study, we also investigated the effect of MHD on HUVECs. In the CCK-8 and scratch assays, MHD promoted HUVECs proliferation and migration. Previous studies have also shown that some of the components of MHD, including *P. villosa* (Cao *et al.*, 2013), *C. officinalis* (Jeon *et al.*, 2010) and *Astragalus* (Lai *et al.*, 2014), stimulate HUVEC proliferation and migration and increase HUVECs viability, with which our results were consistent. By western blotting, we demonstrated that MHD promoted VEGF secretion and activated the PI3K/Akt signaling pathway in both a concentration-dependent and time-dependent manner. One of the active ingredients of MHD, *Astragalus polysaccharides*, has been reported to promote vascular endothelial cell proliferation and repair by activating the PI3K/Akt signaling pathway (Zhang *et al.*, 2016b). Additionally, astragaloside IV was also observed to display an angiogenic effect on endothelial cells, which was reversed by LY294002 (Zhang *et al.*, 2011). Similarly, we also used LY294002 to inhibit the PI3K/Akt signaling pathway and found that PI3K, p-Akt, and p-eNOS were significantly reduced in the MHD+LY294002 group compared with alone MHD group. This indicated that the MHD promotion of HUVECs proliferation depends on the activation of the PI3K/Akt signaling pathway.

While MHD is effective in clinical application, it is, however, a compound composed of a variety of natural medicinal plants. Therefore, the VEGF/PI3K/Akt signaling pathway may not be the only mechanism of its effect on promoting wound healing. Further potential molecular mechanisms need to be investigated. Besides, the limited number of rats used is also a shortage in our study. More animals should be considered in the following research.

CONCLUSIONS

This study showed that MHD significantly promotes wound healing by activating the VEGF/PI3K/Akt signaling pathway. Our study not only helps to explain the mechanism of MHD, but it also provides ideas for the development of new methods to improve wound healing.

Declarations

Availability of data and materials. All data generated or analysed during this study are included in this published article and its supplementary information files.

Acknowledgements. We thank all lab staff for their contributions to this article and the animals sacrificed in this experiment.

Author Contributions. Xiang Xu and Yang Chen performed the cell experiments and wrote the manuscript; Wei-hua Yang and Chun-yu Zhang performed the animal experiments; Yijia Cheng and Jin-gen Lu analyzed the data; Zhi-wei Miao and Ning He designed the research; and all authors proofread and approved the final manuscript.

Competing interests. The authors declare that they have no competing interests.

REFERENCES

Amin ZA, Ali HM, Alshawsh MA, Darvish PH, Abdulla MA (2015) Application of *Antrodia camphorata* promotes rat's wound healing *in vivo* and facilitates fibroblast cell proliferation *in vitro*. *Evid Based Complement Alternat Med* **2015**: 317693. https://doi.org/10.1155/2015/317693

Barrientos S, Stojadinovic O, Golinko MS, Brem H, Tomic-Canic M (2008) Growth factors and cytokines in wound healing. *Wound Repair Regen* **16**: 585–601. https://doi.org/10.1111/j.1524-475X.2008.00410.x

Breen EC (2007) VEGF in biological control. *J Cell Biochem* **102**: 1358–1367. https://doi.org/10.1002/jcb.21579

Cao G, Cai H, Cai B, Tu S (2013) Effect of 5-hydroxymethylfurfural derived from processed *Cornus officinalis* on the prevention of high glucose-induced oxidative stress in human umbilical vein endothelial cells and its mechanism. *Food Chem* **140**: 273–279. https://doi.org/10.1016/j.foodchem.2012.11.143

Chen X, Peng LH, Li N, Li QM, Li P, Fung KP, Leung PC, Gao JQ (2012) The healing and anti-scar effects of astragaloside IV on the wound repair *in vitro* and *in vivo*. *J Ethnopharmacol* **139**: 721–727. https://doi.org/10.1016/j.jep.2011.11.035

Cui MD, Pan ZH, Pan LQ (2017) Danggui buxue extract-loaded liposomes in thermosensitive gel enhance *in vivo* dermal wound healing *via* activation of the VEGF/PI3K/Akt and TGF-beta/Smads signaling pathway. *Evid Based Complement Alternat Med* **2017**: 8407249. https://doi.org/10.1155/2017/8407249

D'Alessio A, Moccia F, Li JH, Micera A, Kyriakides TR (2015) Angiogenesis and vasculogenesis in health and disease. *Biomed Res Int* **2015**: 126582. https://doi.org/10.1155/2015/126582

Eming SA, Martin P, Tomic-Canic M (2014) Wound repair and regeneration: mechanisms, signaling, and translation. *Sci Transl Med* **6**: 265sr266. https://doi.org/10.1126/scitranslmed.3009337

Eremina V, Quaggin SE (2004) The role of VEGF-A in glomerular development and function. *Curr Opin Nephrol Hypertens* **13**: 9–15. https://doi.org/10.1097/00041552-200401000-00002

Ewald F, Norz D, Grottke A, Hofmann BT, Nashan B, Jucker M (2014) Dual Inhibition of PI3K-AKT-mTOR- and RAF-MEK-ERK-signaling is synergistic in cholangiocarcinoma and reverses acquired resistance to MEK-inhibitors. *Invest New Drugs* **32**: 1144–1154. https://doi.org/10.1007/s10637-014-0149-7

Frykberg RG, Banks J (2015) Challenges in the treatment of chronic wounds. *Adv Wound Care (New Rochelle)* **4**: 560–582. https://doi.org/10.1089/wound.2015.0635

Gurtner GC, Werner S, Barrandon Y, Longaker MT (2008) Wound repair and regeneration. *Nature* **453**: 314–321. https://doi.org/10.1038/nature07039

Heyer K, Herberger K, Protz K, Glaeske G, Augustin M (2016) Epidemiology of chronic wounds in Germany: Analysis of statutory health insurance data. *Wound Repair Regen* **24**: 434–442. https://doi.org/10.1111/wrr.12387

Hoke GD, Ramos C, Hoke NN, Crossland MC, Shawler LG, Boykin JV (2016) Atypical diabetic foot ulcer keratinocyte protein signaling correlates with impaired wound healing. *J Diabetes Res* **2016**: 1586927. https://doi.org/10.1155/2016/1586927

Jeon J, Lee J, Kim C, An Y, Choi C (2010) Aqueous extract of the medicinal plant *Patrinia villosa* Juss. induces angiogenesis *via* activation of focal adhesion kinase. *Microvasc Res* **80**: 303–309. https://doi.org/10.1016/j.mvr.2010.05.009

Lai PK, Chan JY, Kwok HF, Cheng L, Yu H, Lau CP, Leung PC, Fung KP, Lau CB (2014) Induction of angiogenesis in zebrafish embryos and proliferation of endothelial cells by an active fraction isolated from the root of *Astragalus membranaceus* using bioassay-

guided fractionation. *J Tradit Complement Med* **4**: 239–245. https://doi.org/10.4103/2225-4110.139109
Landen NX, Li D, Stahle M (2016) Transition from inflammation to proliferation: a critical step during wound healing. *Cell Mol Life Sci* **73**: 3861–3885. https://doi.org/10.1007/s00018-016-2268-0
Lanza F, Healy L, Sutherland DR (2001) Structural and functional features of the CD34 antigen: an update. *J Biol Regul Homeost Agents* **15**: 1–13
Lee SH, Zahoor M, Hwang JK, Min do S, Choi KY (2012) Valproic acid induces cutaneous wound healing *in vivo* and enhances keratinocyte motility. *PLoS One* **7**: e48791. https://doi.org/10.1371/journal.pone.0048791
Lertkiatmongkol P, Liao D, Mei H, Hu Y, Newman PJ (2016) Endothelial functions of platelet/endothelial cell adhesion molecule-1 (CD31) *Curr Opin Hematol* **23**: 253–259. https://doi.org/10.1097/MOH.0000000000000239
Li T, Wang G (2014) Computer-aided targeting of the PI3K/Akt/mTOR pathway: toxicity reduction and therapeutic opportunities. *Int J Mol Sci* **15**: 18856–18891. https://doi.org/10.3390/ijms151018856
Li Y, Wang S, Huang R, Huang Z, Hu B, Zheng W, Yang G, Jiang X (2015) Evaluation of the effect of the structure of bacterial cellulose on full thickness skin wound repair on a microfluidic chip. *Biomacromolecules* **16**: 780–789. https://doi.org/10.1021/bm501680s
Li Y, Zhu H, Wei X, Li H, Yu Z, Zhang H, Liu W (2017) LPS induces HUVEC angiogenesis *in vitro* through miR-146a-mediated TGF-beta1 inhibition. *Am J Transl Res* **9**: 591–600
Liang CC, Park AY, Guan JL (2007) *In vitro* scratch assay: a convenient and inexpensive method for analysis of cell migration *in vitro*. *Nat Protoc* **2**: 329–333. https://doi.org/10.1038/nprot.2007.30
Majewska I, Gendaszewska-Darmach E (2011) Proangiogenic activity of plant extracts in accelerating wound healing – a new face of old phytomedicines. *Acta Biochim Pol* **58**: 449–460
Olsson AK, Dimberg A, Kreuger J, Claesson-Welsh L (2006) VEGF receptor signalling – in control of vascular function. *Nat Rev Mol Cell Biol* **7**: 359–371. https://doi.org/10.1038/nrm1911
Optimal Care of Chronic, Non-Healing, Lower Extremity Wounds: A Review of Clinical Evidence and Guidelines [Internet] (20113) Ottawa (ON): Canadian Agency for Drugs and Technologies in Health
Peng H, Zhang Q, Li J, Zhang N, Hua Y, Xu L, Deng Y, Lai J, Peng Z, Peng B, Chen M, Peng S, Kuang M (2016a) Apatinib inhibits VEGF signaling and promotes apoptosis in intrahepatic cholangiocarcinoma. *Oncotarget* **7**: 17220–17229. https://doi.org/10.18632/oncotarget.7948
Peng S, Zhang Y, Peng H, Ke Z, Xu L, Su T, Tsung A, Tohme S, Huang H, Zhang Q, Lencioni R, Zeng Z, Peng B, Chen M, Kuang M (2016b) Intracellular autocrine VEGF signaling promotes EBDC cell proliferation, which can be inhibited by Apatinib. *Cancer Lett* **373**: 193–202. https://doi.org/10.1016/j.canlet.2016.01.015
Richmond NA, Maderal AD, Vivas AC (2013) Evidence-based management of common chronic lower extremity ulcers. *Dermatol Ther* **26**: 187–196. https://doi.org/10.1111/dth.12051
Shinde AV, Humeres C, Frangogiannis NG (2017) The role of alpha-smooth muscle actin in fibroblast-mediated matrix contraction and remodeling. *Biochim Biophys Acta Mol Basis Dis* **1863**: 298–309. https://doi.org/10.1016/j.bbadis.2016.11.006
Shiojima I, Walsh K (2002) Role of Akt signaling in vascular homeostasis and angiogenesis. *Circ Res* **90**: 1243–1250. https://doi.org/10.1161/01.res.0000022200.71892.9f
Simons M, Gordon E, Claesson-Welsh L (2016) Mechanisms and regulation of endothelial VEGF receptor signalling. *Nat Rev Mol Cell Biol* **17**: 611–625. https://doi.org/10.1038/nrm.2016.87
Somanath PR, Razorenova OV, Chen J, Byzova TV (2006) Akt1 in endothelial cell and angiogenesis. *Cell Cycle* **5**: 512–518. https://doi.org/10.4161/cc.5.5.2538
Squarize CH, Castilho RM, Bugge TH, Gutkind JS (2010) Accelerated wound healing by mTOR activation in genetically defined mouse models. *PLoS One* **5**: e10643. https://doi.org/10.1371/journal.pone.0010643
Terman BI, Dougher-Vermazen M, Carrion ME, Dimitrov D, Armellino DC, Gospodarowicz D, Bohlen P (1992) Identification of the KDR tyrosine kinase as a receptor for vascular endothelial cell growth factor. *Biochem Biophys Res Commun* **187**: 1579–1586. https://doi.org/10.1016/0006-291x(92)90483-2
Xu D, Ma Y, Zhao B, Li S, Zhang Y, Pan S, Wu Y, Wang J, Wang D, Pan H, Liu L, Jiang H (2014) Thymoquinone induces G2/M arrest, inactivates PI3K/Akt and nuclear factor-kappaB pathways in human cholangiocarcinomas both *in vitro* and *in vivo*. *Oncol Rep* **31**: 2063–2070. https://doi.org/10.3892/or.2014.3059
Yuan X, Han L, Fu P, Zeng H, Lv C, Chang W, Runyon RS, Ishii M, Han L, Liu K, Fan T, Zhang W, Liu R (2018) Cinnamaldehyde accelerates wound healing by promoting angiogenesis *via* up-regulation of PI3K and MAPK signaling pathways. *Lab Invest* **98**: 783–798. https://doi.org/10.1038/s41374-018-0025-8
Zhang J, Chen C, Hu B, Niu X, Liu X, Zhang G, Zhang C, Li Q, Wang Y (2016a) Exosomes derived from human endothelial progenitor cells accelerate cutaneous wound healing by promoting angiogenesis through Erk1/2 signaling. *Int J Biol Sci* **12**: 1472–1487. https://doi.org/10.7150/ijbs.15514
Zhang L, Liu Q, Lu L, Zhao X, Gao X, Wang Y (2011) Astragaloside IV stimulates angiogenesis and increases hypoxia-inducible factor-1alpha accumulation *via* phosphatidylinositol 3-kinase/Akt pathway. *J Pharmacol Exp Ther* **338**: 485–491. https://doi.org/10.1124/jpet.111.180992
Zhang X, Yao K, Ren L, Chen T, Yao D (2016b) Protective effect of *Astragalus* polysaccharide on endothelial progenitor cells injured by thrombin. *Int J Biol Macromol* **82**: 711–718. https://doi.org/10.1016/j.ijbiomac.2015.09.051
Zhang Y, Hu G, Lin HC, Hong SJ, Deng YH, Tang JY, Seto SW, Kwan YW, Waye MM, Wang YT, Lee SM (2009) Radix *Astragali* extract promotes angiogenesis involving vascular endothelial growth factor receptor-related phosphatidylinositol 3-kinase/Akt-dependent pathway in human endothelial cells. *Phytother Res* **23**: 1205–1213. https://doi.org/10.1002/ptr.2479
Zhao B, Zhang X, Han W, Cheng J, Qin Y (2017) Wound healing effect of an *Astragalus membranaceus* polysaccharide and its mechanism. *Mol Med Rep* **15**: 4077–4083. https://doi.org/10.3892/mmr.2017.6488
Zielins ER, Brett EA, Luan A, Hu MS, Walmsley GG, Paik K, Senarath-Yapa K, Atashroo DA, Wearda T, Lorenz HP, Wan DC, Longaker MT (2015) Emerging drugs for the treatment of wound healing. *Expert Opin Emerg Drugs* **20**: 235–246. https://doi.org/10.1517/14728214.2015.1018176